Design of fluorescently tagged poly(alkyl cyanoacrylate) nanoparticles for human brain endothelial cell imaging†

Davide Brambilla,[a] Julien Nicolas,*[a] Benjamin Le Droumaguet,[a] Karine Andrieux,*[a] Véronique Marsaud,[a] Pierre-Olivier Couraud[bc] and Patrick Couvreur[a]

Received (in Cambridge, UK) 17th November 2009, Accepted 21st January 2010
First published as an Advance Article on the web 4th February 2010
DOI: 10.1039/b924028d

Rhodamine B-tagged poly(alkyl cyanoacrylate) amphiphilic copolymers have been synthesised, characterised and successfully used to prepare fluorescent nanoparticles for human brain endothelial cell imaging, allowing their uptake and intracellular trafficking to be finely observed.

The medical application of nanotechnologies, often termed nanomedicine, has witnessed a crucial impulse with the development of various types of drug-carrier nanodevices.[1] Among suitable nanocarriers for drug delivery purposes, nanoparticles based on biodegradable poly(alkyl cyanoacrylate) (PACA) (co)polymers have appeared as an established technology for colloidal nanomedicine.[2] Since their introduction in the field of pharmacology, PACA drug carriers have indeed demonstrated significant results in multiple pathologies, well-reviewed in the recent literature.[3]

However, one of the major drawbacks of PACA compared to other biopolymers is the very high reactivity of cyanoacrylate monomers that hampers easy access to well-defined, complex macromolecular architectures and/or functionalised materials.[2] Herein, we report a simple strategy for the synthesis of fluorescently tagged PEGylated nanoparticles and their application to *in vitro* imaging. A convenient strategy to prepare fluorescent nanoparticles is usually to encapsulate a lipophilic dye during the self-assembly process of the corresponding amphiphilic copolymer. However, potential problems may appear by using this approach: (i) as recently highlighted,[4] the fluorescent dye may leak out from the nanoparticles leading to wrong/inaccurate interpretations of confocal fluorescence images regarding the localisation of the nanoparticles due to cell membrane affinity of lipophilic dyes; (ii) the so-called burst effect, corresponding to the surface adsorbed fraction of the dye which is quickly released from the nanoparticles, may lead to an overestimation of the fluorescence intensity in a particular area whereas the nanoparticles are not yet biodegraded; (iii) if a drug has to be encapsulated inside nanoparticles, the co-encapsulation of the fluorescent dye may alter the encapsulation yield of the drug. As a consequence, a fluorescent tag covalently attached to the nanoparticles is highly preferable and would fill in a crucial gap in the field of PACA-based nanoparticles for drug delivery and cell imaging.

With this view, our strategy was to incorporate the fluorophore during the synthesis of an amphiphilic PACA copolymer, by tandem Knoevenagel condensation–Michael addition reaction with hexadecyl cyanoacetate (HDCA), methoxypoly(ethylene glycol) cyanoacetate (MePEGCA) and a small amount of a cyanoacetate derivative based on the desired fluorescent dye (Scheme 1).

Among the possible fluorescent dyes available for fluorescence detection, a rhodamine B derivative was selected. Rhodamine-based fluorescent tags are indeed widely used in the field of biomedical research as they offer a combination of advantageous properties such as a rather high water-solubility, a good photostability, a high extinction coefficient and a high quantum yield. Besides, emission wavelengths of rhodamine-derived fluorescent dyes are higher than those commonly associated with the autofluorescence of cells.[5] A rhodamine B tertiary amide bearing a hydroxyl group[6] was readily transformed into the corresponding cyanoacetate derivative by a DCC-assisted coupling reaction.† This synthetic route was chosen because rhodamine tertiary amides avoid intramolecular cyclisation (which would result in a loss of fluorescence) and fluorescence emission is retained over a broad pH range.[6] The synthesis of rhodamine B cyanoacetate (RCA) was confirmed by ^{1}H and ^{13}C NMR spectroscopy as well as by ESI-MS.† Synthesis of several fluorescent rhodamine B-containing P(HDCA-*co*-RCA-*co*-MePEGCA) copolymers was then undertaken with different RCA initial amounts.

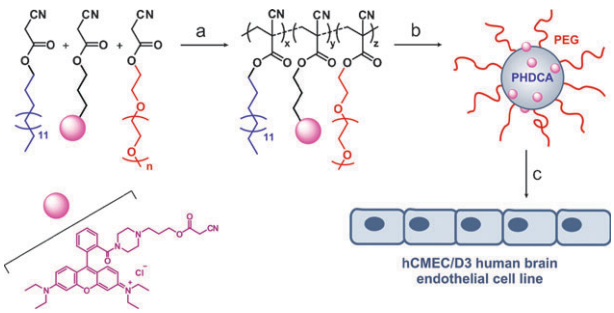

Scheme 1 Design of fluorescent P(HDCA-*co*-RCA-*co*-MePEGCA) copolymers (**C*i***) and nanoparticles (**N*i***) for cell imaging (i = 1–3). *Reagents and conditions*: (a) $[HDCA]_0/[MePEGCA]_0$ = 4 : 1, $[RCA]_0$ = 4.1, 0.85 or 0.16 mol%, formaldehyde, pyrrolidine, EtOH/CH_2Cl_2, 25 °C, 24 h; (b) acetone/H_2O; (c) incubation with hCMEC/D3 cells.

[a] *Laboratoire de Physico-Chimie, Pharmacotechnie et Biopharmacie, Université Paris-Sud, UMR CNRS 8612, Faculté de Pharmacie, 5 rue Jean-Baptiste Clément, F-92296 Châtenay-Malabry cedex, France. E-mail: julien.nicolas@u-psud.fr, karine.andrieux@u-psud.fr; Fax: +33 1 46 83 59 46; Tel: +33 1 46 83 58 53*
[b] *Institut Cochin, Université Paris Descartes, UMR CNRS 8104, 75014 Paris, France*
[c] *Inserm, U567, Paris, France*

† Electronic supplementary information (ESI) available: Experimental details and CLSM images. See DOI: 10.1039/b924028d

Three of these copolymers are discussed here: copolymers **C1**, **C2** and **C3**, corresponding, respectively to 4.10, 0.85 and 0.16 mol% of RCA in the initial cyanoacetate feed. The fluorescent copolymers were analysed by ^{1}H NMR spectroscopy and showed an excellent correlation with the expected structure (Fig. S1).† Size exclusion chromatography showed low number-average molar masses, M_n, with high polydispersity indexes (Table S1)† due to the significant amount of low-molar mass amphiphilic oligomers, commonly observed for this kind of reaction.[7,8] No influence of the initial amount of RCA over the copolymerisation process was observed.

Well-defined nanoparticles were formed by self-assembly in aqueous medium and characterised by DLS and ζ-potential measurements as functions of the RCA initial amount and time (Table S1 and Fig. S2).† In all cases, stable nanoparticles were obtained with average diameters in the 115–125 nm range together with narrow particle size distributions. ζ-potential measurements showed negative values from −30.9 to −40.6 mV. Besides, nanoparticle diameters and surface charge remained constant over time in aqueous solution at 37 °C, thus confirming their excellent stability at a temperature relevant for biomedical assays. Therefore, all these characteristics make them suitable candidates for drug delivery purposes and cell imaging.

The presence of different amounts of RCA in the copolymers and associated nanoparticles could be readily perceived under visible light and UV excitation at 365 nm (Fig. 1). Fluorescent properties of the materials were then thoroughly studied by fluorescence spectroscopy (Fig. 1 and S3–S7).† Emission and excitation wavelengths of the copolymers and nanoparticles were determined. For instance for copolymer **C2**, λ_{ex} = 563 nm and λ_{em} = 583 nm, with a Stokes shift of 20 nm, in good agreement with the spectral properties of rhodamine B-tertiary amide derivatives.[6] No significant change was observed upon self-assembly as λ_{ex} = 568 nm and λ_{em} = 583 nm were recorded for nanoparticles **N2**. Besides, for a given copolymer (or nanoparticle) concentration, the fluorescence intensity decreased when decreasing the initial amount of RCA in the starting cyanoacetate mixture (Fig. 1).

Eventually, the evolution of the fluorescence intensity of copolymer solutions and resulting nanoparticle suspensions was recorded as a function of the concentration, allowing linear and curved parts to be determined (Fig. S7),† which is useful for fluorescence intensity-based calculations. Whatever

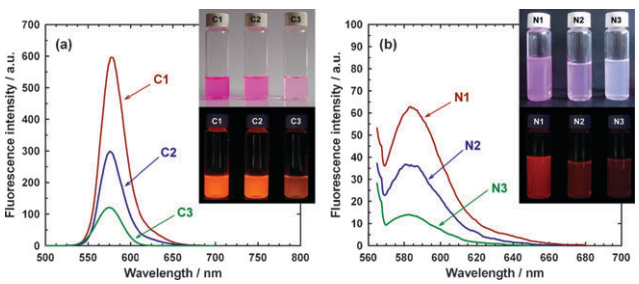

Fig. 1 Fluorescence emission spectra of P(HDCA-*co*-RCA-*co*-MePEGCA) copolymer solutions in $CHCl_3$ at 0.1 mg mL^{-1} (a) and of resulting nanoparticle suspensions in water at 0.1 mg mL^{-1} (b). Inserts: pictures of copolymer solutions (left) and nanoparticle suspensions (right) under visible light or under UV excitation at 365 nm.

the nature of the copolymer and associated nanoparticles, linear evolutions of fluorescence intensity *vs.* concentration were observed up to rather high concentrations.

Rhodamine B-tagged PACA nanoparticles were then employed for *in vitro* imaging studies on the hCMEC/D3 human brain endothelial cell line, which has been validated as a unique *in vitro* model of the human blood–brain barrier (BBB).[9] Prior to imaging studies, cell viability assays were performed in order to determine the cytotoxicity of the P(HDCA-*co*-RCA-*co*-MePEGCA) nanoparticles on hCMEC/D3 cells. No statistical difference in cytotoxicity was observed between nanoparticles containing an increasing amount of rhodamine B (Fig. S10).† Similarly to non-fluorescent P(HDCA-*co*-MePEGCA) nanoparticles, no significant cytotoxicity was obtained until a concentration of 30 μg mL^{-1}.

Confocal laser scanning microscopy (CLSM) was then employed for *in vitro* imaging studies. Upon microscope observation, the fluorescent nanoparticles in water appeared as small, well-defined, fluorescent spots displaying typical Brownian motion (Fig. S11).† After a 12 h incubation period of hCMEC/D3 cells with fluorescent nanoparticles (**N1**), cells were washed with fresh cell culture medium in order to remove adsorbed nanoparticles and observed by CLSM. Nomarski contrast images showed a typical fibroblast shape for the cells with no morphological alteration, thus supporting the absence of cytotoxicity as previously shown by cell viability assays (this observation was made on the basis of numerous images randomly taken from the cell monolayer). Fluorescence images superimposed on the Nomarski images showed intense and fine fluorescence spots accumulated within the cells and especially around the nuclei (Fig. 2a–c). This observation suggested that the mechanism by which nanoparticles entered the cells was governed by endocytosis since fluorescence was localised into vesicles. However, according to their proximity to the nuclei, those vesicles are highly supposed to be late endosomes (Fig. 2d). These results confirmed previous observations with primary cultures of rat brain endothelial cells showing that P(HDCA-*co*-MePEGCA) nanoparticles were able to penetrate by endocytosis.[10]

As long as poly(alkyl cyanoacrylate) nanoparticles are known to be biodegradable by enzymatic degradation *via* hydrolysis of ester functions,[2] it was important to assess that the observed fluorescence intensity was coming from the fluorescent nanoparticles and not from free rhodamine B alcohol (released after hydrolysis). After 8 h incubation of fluorescent nanoparticles at different concentrations with Fischer rat plasma at 37 °C, only 11–14% of fluorescence loss was measured (Fig. S12),† in very good agreement with the *in vitro* biodegradation profile of non-fluorescent P(HDCA-*co*-PEGCA) nanoparticles.[11] This result also showed that the presence of rhodamine B cyanoacetate units in the macromolecular structure did not alter the degradation profile of the nanoparticles.

Under identical experimental conditions and acquisition settings (detector gain: 535, laser power: 57%), a lower amount of rhodamine dye covalently linked to the nanoparticles resulted in a decrease of fluorescence intensity. Indeed, only faint fluorescent areas were noticed for nanoparticles **N3** (Fig. S13).† Nevertheless, by increasing the detector gain up

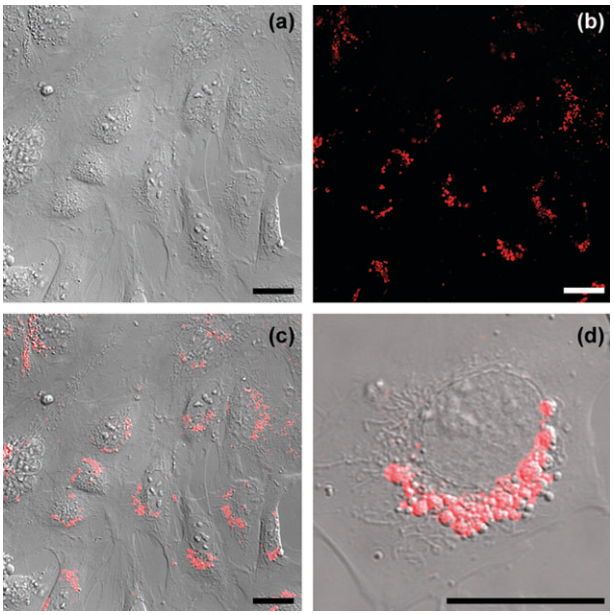

Fig. 2 hCMEC/D3 human brain endothelial cells Nomarski image (a), confocal microscopy image (b) and fluorescence image superimposed on hCMEC/D3 human brain endothelial cell Nomarski image after incubation with fluorescent P(HDCA-*co*-RCA-*co*-MePEGCA) nanoparticles **N1** for 12 h and subsequent washing of the medium (c). Enlarged picture (d). Scale bars = 20 μm.

to 700 together with a laser power at 65%, intense fluorescence spots appeared around cell nuclei. Therefore, tuning the amount of fluorescent dye attached to the nanoparticles together with adjusting acquisition settings allowed great flexibility regarding *in vitro* imaging.

Concerning BBB crossing, important work remains to be done as long as several crucial mechanisms are still unknown such as those of intracellular trafficking and exocytosis. In order to determine whether these fluorescent nanoparticles are suitable for such investigations, real-time confocal fluorescence microscopy observations were performed. While focusing on a dividing cell, the fine fluorescence signal coming from the nanoparticles allowed their intracellular progression to be accurately followed. Indeed, we clearly observed that nanoparticles were trafficked from the polar extremity during metaphase/anaphase (Fig. 3a) to the midbody area during telophase, where the fluorescence exhibited a filament-like clustered structure (Fig. 3b). Thus, this new synthetic tool allows intracellular events to be finely monitored and could give new insights into intracellular mechanisms.

Finally, this approach is very versatile and can be applied to other fluorescent dyes after suitable modification to insert the cyanoacetate moiety. This was exemplified by the synthesis of dansyl cyanoacetate (DCA, Scheme S2)† and the preparation of the corresponding P(HDCA-*co*-DCA-*co*-MePEGCA) fluorescent nanoparticles **N4** (see ESI).†

In summary, in order to circumvent the drawbacks usually encountered with the use of fluorescent dyes encapsulated into nanoparticles, an original and versatile strategy has been developed to prepare fluorescent nanoparticles where a hydrophilic dye based on rhodamine B has been covalently linked to P(HDCA-*co*-MePEGCA) amphiphilic copolymers. The resulting fluorescently tagged nanoparticles demonstrated suitable characteristics for *in vitro* imaging of human brain endothelial cells and their fluorescence signal was found to be extremely accurate, as opposed to a diffuse signal obtained when a lipophilic dye is encapsulated. This allowed their uptake and intracellular trafficking to be finely observed. These results also open the door to further studies related to endocytosis during mitosis which represents an important aspect of cellular biology.

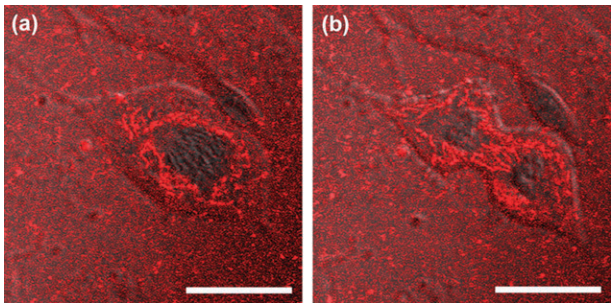

Fig. 3 Fluorescence images (red) superimposed on hCMEC/D3 human brain endothelial cell Nomarski images viewed from the top cell surface recorded at various times after incubation with fluorescent P(HDCA-*co*-RCA-*co*-MePEGCA) nanoparticles (**N1**): 8.5 min (a) and 18 min (b). Scale bars = 20 μm.

The authors thank Valérie Nicolas (Plateforme Imagerie Cellulaire, IFR 141) for her kind help with the CLSM. The research leading to these results has received funding from the European Community's Seventh Framework Programme (FP7/2007-2013) under grant agreement no 212043. The CNRS is also warmly acknowledged for financial support.

Notes and references

1 O. C. Farokhzad and R. Langer, *ACS Nano*, 2009, **3**, 16; S. E. Erb, *Drug Delivery Syst.*, 2009, **24**, 63.
2 J. Nicolas and P. Couvreur, *Wiley Interdiscip. Rev. Nanomed. Nanobiotechnol.*, 2009, **1**, 111.
3 C. Vauthier, C. Dubernet, E. Fattal, H. Pinto-Alphandary and P. Couvreur, *Adv. Drug Delivery Rev.*, 2003, **55**, 519.
4 P. Xu, E. Gullotti, L. Tong, C. B. Highley, D. R. Errabelli, T. Hasan, J.-X. Cheng, D. S. Kohane and Y. Yeo, *Mol. Pharmaceutics*, 2009, **6**, 190.
5 R. C. Benson, R. A. Meyer, M. E. Zaruba and G. M. McKhann, *J. Histochem. Cytochem.*, 1979, **27**, 44.
6 T. Nguyen and M. B. Francis, *Org. Lett.*, 2003, **5**, 3245; J. Nicolas, V. San Miguel, G. Mantovani and D. M. Haddleton, *Chem. Commun.*, 2006, 4697.
7 M. T. Peracchia, D. Desmaële, P. Couvreur and J. d'Angelo, *Macromolecules*, 1997, **30**, 846.
8 J. Nicolas, F. Bensaid, D. Desmaële, M. Grogna, C. Detrembleur, K. Andrieux and P. Couvreur, *Macromolecules*, 2008, **41**, 8418.
9 L. Cucullo, P. O. Couraud, B. Weksler, I. A. Romero, M. Hossain, E. Rapp and D. Janigro, *J. Cereb. Blood Flow Metab.*, 2008, **28**, 312.
10 H. R. Kim, S. Gil, K. Andrieux, V. Nicolas, M. Appel, H. Chacun, D. Desmaële, F. Taran, D. Georgin and P. Couvreur, *Cell. Mol. Life Sci.*, 2007, **64**, 356.
11 I. Brigger, J. Morizet, G. Aubert, H. Chacun, M. J. Terrier-Lacombe, P. Couvreur and G. Vassal, *J. Pharmacol. Exp. Ther.*, 2002, **303**, 928.

